Monobit Digital Receivers for QPSK: Design, Analysis and Performance

Zhiyong Wang, *Student Member, IEEE,* Huarui Yin, *Member, IEEE,*
Wenyi Zhang, *Senior Member, IEEE,* and Guo Wei

Abstract

Future communication system requires large bandwidth to achieve high data rate up to multigigabit/sec, which makes analog-to-digital (ADC) become a key bottleneck for the implementation of digital receivers due to its high complexity and large power consumption. Therefore, monobit receivers for BPSK have been proposed to address this problem. In this work, QPSK modulation is considered for higher data rate. First, the optimal receiver based on monobit ADC with Nyquist sampling is derived, and its corresponding performance in the form of deflection ratio is calculated. Then a suboptimal but more practical monobit receiver is obtained, along with iterative demodulation and small sample removal. The effect of the imbalances between the In-phase (I) and Quadrature-phase (Q) branches, including the amplitude and phase imbalances, is carefully investigated too. To combat the performance loss caused by IQ imbalances, monobit receivers based on double training sequences are proposed. Numerical simulations show that the low-complexity suboptimal receiver suffers only 3dB signal to noise ratio (SNR) loss in AWGN channels and 1dB SNR loss in multipath static channels compared with the matched filter based monobit receiver with full channel state information (CSI). The impact of the phase difference between the transmitter and receiver is presented. It is observed that the performance degradation caused by the amplitude imbalance is negligible. Receivers based on double training sequences can efficiently compensate the performance loss in AWGN channel. Thanks to the diversity offered by the multipath, the effect of imbalances on monobit receivers in fading channels is slight.

Index Terms

Z. Wang, H. Yin, W. Zhang and G. Wei are with Department of Electronic Engineering and Information Science, University of Science and Technology of China, Hefei, China. (e-mail: zywangzy@gmail.com)

This research has been funded in part by the National Science Foundation of China under Grant No. 60802008.

Analog-to-digital conversion, deflection ratio, impulse radio, imbalance, monobit, QPSK modulation, ultra-wideband

I. INTRODUCTION

To achieve high data rate, future communication systems require large bandwidth. One typical example of such systems is ultra-wideband (UWB) communication, where the bandwidth could be 1 GHz or more. Another example is communication in the 60 GHz band [1], which aims to achieve multigigabit/sec. Due to the significant large bandwidth, it is a huge challenge to design a sophisticated digital receiver with implementation simplicity and economic efficiency.

When the received signals of the high-rate high bandwidth systems are processed digitally, the analog-to-digital converter (ADC) becomes a key bottleneck. Since the power consumption of ADC is proportional to 2^b, where b is the bit number of the ADC [2], high-speed high-resolution ADC is power-hungry and costly. Therefore, single-bit or monobit ADC has attracted great attention in recent years, e.g., [3], [4]. As it can be simply realized by fast comparator, the monobit ADC can reach tens of Gsps sampling rate with very low power consumption; see, e.g., [5].

For UWB communication using impulse radio (IR), there have been several transmission strategies before monobit sampling was introduced. These receivers mainly include the matched-filter based coherent receiver which requires accurate synchronization, e.g., [6]; autocorrelation based receivers which employ precise delay device, e.g., [7], [8]; and noncoherent receiver based on energy detection which is insufficient to combat multipath fading, e.g., [9].

A matched-filter based monobit receiver was proposed in [4] for UWB communication. Through correlating the 1-bit sampling output with the ideal noiseless received waveform, the receiver detects the BPSK symbols. However, the requirement for full resolution (FR) ideal received waveform makes it difficult to implement. And just as proved in [10], such receiver is not optimal under Nyquist sampling even with the full resolution received waveform.

The optimal monobit receiver for BPSK was proposed in [10], which turns out to take the form of a linear combiner. By performing a Taylor's expansion of the optimal weights, a suboptimal receiver was also derived in [10]. Besides, some simple but useful tricks such as iterative demodulation and removal of small-weight points were shown to be effective. Compared

with the receiver given by [4], the receiver proposed in [10] is easy to implement and only has a slight performance loss, even without the channel state information (CSI).

To achieve higher data rate, higher order modulations such as QPSK or QAM are taken into consideration. A monobit receiver for standard uniform Phase Shift Keying (PSK) modulation was proposed in [11]. Such receiver employs 'Phase-Quantization' for demodulation, which is realized through multiple 1-bit ADCs preceded by analog multipliers. Compared with the traditional receiver architecture, this receiver is much more complex.

In this paper, we study the design and performance of digital receivers for QPSK under the traditional receiver architecture, based on monobit sampling with a certain over-sampling rate. First, the maximum likelihood (ML) receiver is derived under monobit sampling. And its performance is analyzed in the form of deflection ration (see, e.g., [12]), to simplify the computation. Secondly, the main ideas in [10] are extended here to derive a suboptimal receiver for QPSK. The effect of the phase difference between the transmitter and the receiver is investigated. And the interface with error-control decoder is also obtained. It is shown that the suboptimal receiver without any prior information has only 3dB performance loss compared to the monobit matched-filter with full CSI in additive white Gaussian noise (AWGN) channel under the assumption of perfect timing. In fading channel without inter symbol interference (ISI), the resulting practical receiver has only 3dB loss even compared with the full-resolution matched filter (FRMF), and only has 1dB loss compared to the monobit matched filter.

A limiting issue of practical communication systems is the imbalance between the In-phase (I) and Quadrature-phase (Q) branches when received radio-frequency (RF) signal is down-converted to baseband. Basically, the IQ imbalance is any mismatch between the I and Q branches from the ideal case, including amplitude and phase imbalances elaborated in [13]. Compared to the heterodyne receiver, the direct conversion RF receiver considered in this paper is effected more seriously by the IQ imbalances [14]. Although this problem is well investigated in traditional system with high-resolution ADC, there has not been much published work to deal with the IQ imbalances under low-precision sampling.

In this paper, we will first introduce a formulation, according to [15], to describe the received signal distorted by the IQ balances. Then, the problems of directly applying the suboptimal monobit receiver to demodulate the received signal with IQ imbalances are discussed. At last, the frame structure and the suboptimal receiver are modified to combat the performance degradation

caused by IQ imbalances. It is shown that the performance degradation caused by amplitude imbalance is negligible in AWGN channel. With phase imbalance, even the matched filter with monobit sampling has a 10^{-2} error floor. The modified receivers proposed, though having an upturn of the BER in the intermediate signal to noise ratio (SNR) region, outperform the matched filter in the high SNR region. Thanks to the diversity offered by multipath, the performance loss in fading channel is negligible.

The rest of the paper is organized as follows. The system model and proposed architecture are presented in the next section. The optimal monobit receiver and its performance in the form of deflection ratio are given in section III. In section IV, a suboptimal but more practical receiver is presented, with discussion on several important practical issues such as channel estimation, effect of phase difference and interface with error-control decoder. Section V discusses the effect of IQ imbalances at the receiver, and modified the frame structure and the suboptimal receiver to combat the performance degradation. Application of the proposed structure to UWB signaling and numerical results are provided in VI. At last, section VII concludes the paper.

II. System Model And Receiver Architecture

The monobit digital receiver we study is depicted in the block diagram in Figure 1. The received QPSK baseband signal is composed of the in-phase component and the quadrature component. Both of them are first filtered by an ideal low pass filter (LPF) of bandwidth B, then sampled and quantized by a 1-bit ADC at Nyquist rate $2B$, respectively. The digitized signals are processed by the digital signal processing (DSP) unit.

In order to get better bit error rate (BER) performance, the Gray coded QPSK modulation is usually employed [16]. Thus, we can write the transmitted signal as

$$s(t) = \sum_{k=0}^{\infty} e^{j\theta(d_{k1},d_{k0})} p_{tr}(t - kT_s) \tag{1}$$

where k is the symbol index, T_s is symbol duration, $d_{k0}, d_{k1} \in \{+1, -1\}$ are the binary data of the kth QPSK symbol, $\theta(x, y)$ is the QPSK modulation function according to Gray coding rules, that is $\theta(1,1) = 0$, $\theta(1,-1) = \pi/2$, $\theta(-1,1) = -\pi/2$, $\theta(-1,-1) = \pi$. p_{tr} is the spectral shaping pulse. Generally, we can assume that both d_{k0} and d_{k1} are equally likely to be ± 1, and they can be either uncoded or coded.

The channel is modeled as a linear time-invariant system with a finite impulse response $h(t)$. In the case of wireless time-varying channel, we assume that within the coherent interval the channel can be modeled as time-invariant. The received signal can be written as $r(t) = s(t) \star h(t) + n(t)$, where $\star$ denotes convolution, and $n(t)$ is AWGN with double-sided power spectral density $N_0/2$. We assume that there is no interference here.

Both of the I and Q components of the received signal are first filtered by an ideal LPF respectively. The bandwidth of the ideal LPF is B, and its impulse response is $p_{rec}(t) = sin(2\pi Bt) / \left(\pi t\sqrt{N_0 B}\right)$. The gain of the LPF, $1/\sqrt{N_0 B}$, is chosen so that the noise variance after sampling will be normalized to one. We define $p_{ref}(t) = p_{tr}(t) \star h(t) \star p_{rec}(t)$ as the reference signal. Assuming that there is no frequency mismatch between the transmitter and the receiver, then the filtered received signal can be written as follows

$$r(t) = \sum_{k=0}^{\infty} e^{j(\theta(d_{k1}, d_{k0}) + \varphi)} p_{ref}(t - kT_s) + n'(t) \tag{2}$$

where φ is the phase difference of the local oscillators of the transmitter and the receiver, and $n'(t) = n(t) \star p_{rec}(t)$ is the filtered noise with variance one. The phase difference φ of the local oscillators is a random variable with uniform distribution on $[0, 2\pi]$. From (2), we can derive the in-phase component of the filtered received signal

$$r_I(t) = \sum_{k=0}^{\infty} p_{ref}(t - kT_s) \cos(\theta(d_{k1}, d_{k0}) + \varphi) + n_I(t) \tag{3}$$

And the quadrature component of the filtered received signal can also be given as

$$r_Q(t) = \sum_{k=0}^{\infty} p_{ref}(t - kT_s) \sin(\theta(d_{k1}, d_{k0}) + \varphi) + n_Q(t) \tag{4}$$

The notations $n_I(t)$ and $n_Q(t)$, independent to each other, denote the Gaussian noise of the I and Q branches respectively, and both of them have a variance of $1/2$.

We choose the filter bandwidth B and the sampling period T to be $T = 1/(2B) = T_s/N$, so that the Nyquist rate sampling of the filtered signal is used and every pulse is sampled by N points. Within the kth symbol, we denote the lth sample of the I branch as $r_{I,k,l}$, and the lth sample of the Q branch as $r_{Q,k,l}$. Then we have

$$r_{I,k,l} = \begin{cases} 1, & r_I(kT_s + lT) > 0 \\ -1, & r_I(kT_s + lT) \leq 0 \end{cases} \qquad l = 0, ..., N-1 \tag{5}$$

and

$$r_{Q,k,l}=\begin{cases}1, & r_Q\left(kT_s+lT\right)>0\\ & \qquad\qquad l=0,...,N-1\\ -1, & r_Q\left(kT_s+lT\right)\leq 0\end{cases} \tag{6}$$

We assume the maximum delay spread is significantly smaller than symbol duration T_s so that ISI is negligible. For a fixed symbol index k, we can rewrite (2) as follows

$$r\left(t\right)=\begin{cases}p_{ref}\left(t-kT_s\right)\cos\left(\varphi\right)+j*p_{ref}\left(t-kT_s\right)\sin\left(\varphi\right)+n'\left(t\right), & d_{k1}=1,d_{k0}=1\\ -p_{ref}\left(t-kT_s\right)\sin\left(\varphi\right)+j*p_{ref}\left(t-kT_s\right)\cos\left(\varphi\right)+n'\left(t\right), & d_{k1}=1,d_{k0}=-1\\ p_{ref}\left(t-kT_s\right)\sin\left(\varphi\right)-j*p_{ref}\left(t-kT_s\right)\cos\left(\varphi\right)+n'\left(t\right), & d_{k1}=-1,d_{k0}=1\\ -p_{ref}\left(t-kT_s\right)\cos\left(\varphi\right)-j*p_{ref}\left(t-kT_s\right)\sin\left(\varphi\right)+n'\left(t\right), & d_{k1}=-1,d_{k0}=-1\end{cases} \tag{7}$$

Define

$$\epsilon_{I,l}=Q\left(p_{ref}\left(lT\right)\cos\left(\varphi\right)\right),\quad \epsilon_{Q,l}=Q\left(p_{ref}\left(lT\right)\sin\left(\varphi\right)\right) \tag{8}$$

where $Q\left(\cdot\right)$ is the Q function

$$Q\left(x\right)=\frac{1}{\sqrt{2\pi}}\int_x^{\infty}e^{-\frac{t^2}{2}}dt \tag{9}$$

We can view $\epsilon_{I,l}$ as the error probability for binary transmission of the lth "chip", $p_{ref}\left(lT\right)\cos\left(\varphi\right)$, through AWGN channel. Let $r_{I,l}$ denote the lth sample of the "chip" with one bit resolution, and d denote the binary data, we have

$$P\left(r_{I,l}|d_k\right)=\begin{cases}1-\epsilon_{I,l}, & r_{I,l}=d\\ & \qquad l=0,...,N-1\\ \epsilon_{I,l}, & r_{I,l}\neq d\end{cases} \tag{10}$$

When the binary data d is given, $r_{I,l}$ can be viewed as the result of transmitting d through a binary symmetric channel (BSC) with parameter $\epsilon_{I,l}$. Analogously, we can get a similar result about $\epsilon_{Q,l}$.

Define $\mathbf{r}_k=\left[r_{I,k,0},r_{Q,k,0},...,r_{I,k,N-1},r_{Q,k,N-1}\right]^T$. The digital signal processing unit of the receiver is to detect d_{k0}, d_{k1} based on $\mathbf{r}_k$.

III. Optimal Monobit Receiver Under Nyquist Sampling

In this section, we first derive the optimal detector for (d_{k1},d_{k0}) based on vector $\mathbf{r}_k$, assuming that both the received reference signal $p_{ref}\left(t\right)$ and the phase difference φ are available at the receiver. Then we analyze the uncoded BER performance of the derived optimal monobit receiver.

A. Optimal Monobit Receiver

In communication systems, we commonly assume that d_{k0}, d_{k1} are equally likely to be ± 1. This implies that the optimal detector, based on the digital samples $\mathbf{r}_k$, is the maximum-likelihood (ML) detector, which minimizes the error probability. Thanks to the memoryless property of the AWGN, we have

$$P\left(\mathbf{r}_k|d_{k1},d_{k0}\right)=\prod_{l=0}^{N-1}P\left(r_{I,k,l},r_{Q,k,l}|d_{k1},d_{k0}\right)=\prod_{l=0}^{N-1}P\left(r_{I,k,l}|d_{k1},d_{k0}\right)P\left(r_{Q,k,l}|d_{k1},d_{k0}\right) \quad (11)$$

Then the log-likelihood functions of the kth symbol, denoted by $\Lambda_k^{(opt)}\left(d_{k1},d_{k0}\right)$, are given as follows

$$\begin{aligned}\Lambda_k^{(opt)}\left(d_{k1},d_{k0}\right)=\sum_{l=0}^{N-1}\Bigg\{&\log\left(1+\left(\frac{d_{k1}+d_{k0}}{2}r_{I,k,l}+\frac{d_{k1}-d_{k0}}{2}r_{Q,k,l}\right)\left(1-2\epsilon_{I,l}\right)\right)\\&+\log\left(1-\left(\frac{d_{k1}-d_{k0}}{2}r_{I,k,l}-\frac{d_{k1}+d_{k0}}{2}r_{Q,k,l}\right)\left(1-2\epsilon_{Q,l}\right)\right)\Bigg\}-2N\log 2\end{aligned} \quad (12)$$

And the ML detector is given by

$$\left(\hat{d}_{k1},\hat{d}_{k0}\right)=\arg\max_{d_{k1},d_{k0}=\pm 1}\Lambda_k^{(opt)}\left(d_{k1},d_{k0}\right) \quad (13)$$

B. Performance of Optimal Monobit Receiver

To calculate the uncoded error probability of the optimal ML receiver proposed above, we generally assume that symbol $(d_1=1,d_1=1)$ is transmitted. The symbol index k is suppressed to simplify the notation. A symbol detection error event occurs when $\Lambda\left(d_1=1,d_0=1\right)$ is smaller than any of the other LLR values. Considering the Gray coded QPSK modulation is employed, we can assume that the bit error probability is approximately equal to symbol error probability. Thus, the bit error probability can be given as follows

$$P_e=1-P\left(\Lambda\left(d_1=1,d_0=1\right)=\max_{d_1=\pm 1,d_0=\pm 1}\Lambda\left(d_1,d_0\right)\right) \quad (14)$$

The calculation of (14) can be decomposed. Let $P_e\left(\mathbf{r}\right)$ denote the detection error probability, which is ether 1 or 0, based on a specific digital sample vector $\mathbf{r}$. Then the bit error probability P_e can be calculated as

$$P_e=\sum_{\mathbf{r}}P_e\left(\mathbf{r}\right)P\left(\mathbf{r}\right) \quad (15)$$

However, evaluating (15) obviously needs to sum over 2^{2N} terms, which is extremely complex especially when N is large.

In view of the calculation complexity of the BER performance, some simpler performance criteria are shown to be attractive. Among those, the deflection ratio criterion is one of the most interesting, not only for its simplicity of calculation, but also the equivalence between the ML receiver and the optimum receiver in terms of deflection [12]. Therefore, we will analyze the performance of optimal monobit receiver in terms of deflection ratio in the following.

Define the decision statistic as $\lambda = \Lambda\left(d_1 = 1, d_0 = 1\right)$. According to [12], the deflection ratio under QPSK modulation with monobit sampling is given as

$$D = \frac{\left[E\left(\lambda | d_1 = 1, d_0 = 1\right) - E\left(\lambda | d_1 = 1, d_0 = -1\right)\right]^2}{Var\left(\lambda\right)} \tag{16}$$

After some manipulations, the deflection ratio of the optimal ML receiver is given as follows

$$D = \frac{\left[\sum\limits_{l=0}^{N-1}\left(\left(1-\epsilon_{I,l}-\epsilon_{Q,l}\right) log\frac{1-\epsilon_{I,l}}{\epsilon_{I,l}} + \left(\epsilon_{I,l}-\epsilon_{Q,l}\right)\frac{1-\epsilon_{Q,l}}{\epsilon_{Q,l}}\right)\right]^2}{\sum\limits_{l=0}^{N-1}\frac{\epsilon_{I,l}\left(1-\epsilon_{I,l}\right)+\epsilon_{Q,l}\left(1-\epsilon_{Q,l}\right)}{2}\left(log^2\frac{1-\epsilon_{I,l}}{\epsilon_{I,l}} + log^2\frac{1-\epsilon_{Q,l}}{\epsilon_{Q,l}}\right)} \tag{17}$$

From another perspective, the decision statistic λ can be treated as a Gaussian random variable using a central limit argument, when N is large. Thus, the BER performance can be approximately estimated as $Q\left(\sqrt{D}\right)$, which makes the deflection ratio be a simpler performance criterion. It can be observed that the reception performance will be better if the deflection ratio is bigger.

With the information of the received reference waveform $p_{ref}\left(t\right)$ and the phase difference φ (and hence the channel state information), we can evaluate the deflection ratio of the optimal monobit receiver to obtain a general point of view about its performance.

IV. Practical Monobit Receiver

In the previous section, we have discussed the optimal monobit detector and its performance. However, it is quite difficult to implement such a receiver in practice, since the receiver can get access neither to the precise reference signal $p_{ref}\left(t\right)$ nor to the phase difference φ. Besides, the $\log$ operation in the ML receiver is complex to implement, even by a lookup table. A reference signal estimation based on training sequence is proposed in [17] for BPSK modulation. Unfortunately, it still requires a large lookup table and exhaustive search. The method to recover the reference signal from 1-bit quantized signal by using training symbols in [10] only requires bit-level addition and shift operations, which can be simply realized online. Therefore, the main

ideas to obtain the suboptimal receiver in [10] are extended to the QPSK modulation in this section, and a practical monobit receiver for QPSK modulation is derived. We also give some performance analysis about the resulting receiver.

A. Suboptimal Monobit Receiver

The first skill to be used is the Taylor's expansion. When SNR is small, $\epsilon_{I,l} \approx 0.5$ and $\epsilon_{Q,l} \approx 0.5$. Thus we can perform a first order Taylor's expansion of the $\log$ functions in (12), according to $\log(1+x) \approx 1+x$ when $x \approx 0$. Define $w_{I,l} = 1 - 2\epsilon_{I,l}$ and $w_{Q,l} = 1 - 2\epsilon_{Q,l}$, which are approximately equal to 0 when SNR is small. Considering the constant $-2N\log 2$ in (12) has no effect on the performance of demodulation in the uncoded case, we ignore this constant and derive the following linear approximations of (12)

$$\begin{aligned}\Lambda_k(d_{k1}, d_{k0}) = \sum_{l=0}^{N-1} \Bigg\{ & w_{I,l}\left(\frac{d_{k1}+d_{k0}}{2} r_{I,k,l} + \frac{d_{k1}-d_{k0}}{2} r_{Q,k,l}\right) \\ & - w_{Q,l}\left(\frac{d_{k1}-d_{k0}}{2} r_{I,k,l} - \frac{d_{k1}+d_{k0}}{2} r_{Q,k,l}\right)\Bigg\}\end{aligned} \tag{18}$$

Therefore, in the suboptimal detector given in (13), we replace $\Lambda_k^{(opt)}(d_{k1}, d_{k0})$ by $\Lambda_k(d_{k1}, d_{k0})$.

Due to the monobit quantization, the receiver can not obtain the precise reference signal $p_{ref}(t)$ and the phase difference φ, or equivalently $\epsilon_{I,l}$, $\epsilon_{Q,l}$. Hence, we need to estimate $\epsilon_{I,l}$ and $\epsilon_{Q,l}$, to further estimate $w_{I,l}$ and $w_{Q,l}$. Assume that a sequence of training symbols (say N_t symbols) are used for estimation. Without loss of generality, we assume that all symbols in the training sequence are $(d_1 = 1, d_0 = 1)$. Then the ML estimate of $w_{I,l}$ can be given as

$$\hat{w}_{I,l} = \frac{1}{N_t}\sum_{k=0}^{N_t-1} r_{I,k,l}, \quad 0 \le l < N-1 \tag{19}$$

Similarly, the ML estimate of $w_{Q,l}$ is as follows

$$\hat{w}_{Q,l} = \frac{1}{N_t}\sum_{k=0}^{N_t-1} r_{Q,k,l}, \quad 0 \le l < N-1 \tag{20}$$

Replacing $w_{I,l}$ and $w_{Q,l}$ in (18) with $\hat{w}_{I,l}$ and $\hat{w}_{Q,l}$ respectively, the practical monobit receiver without prior CSI is derived.

It is reasonable to plug $\hat{w}_{I,l}$ and $\hat{w}_{Q,l}$ into (12) and obtain a ML receiver without prior CSI. However, the $\log$ operation in the ML receiver will significantly increase the complexity. Furthermore, the robustness of such receiver is poor when SNR is relatively large, since a small

estimation error will lead to a large error in detection. For these reasons, we will only focus the suboptimal but more robust monobit receiver when perfect CSI is unavailable.

In [10], iteration is proved to be efficient for BPSK demodulation. The main idea of such iterative demodulation is using previous decided symbols to refine the weight estimation. This can also be applied to the QPSK reception. First, the iterative demodulation algorithm estimates the wights $\hat{w}_{I,l}$ and $\hat{w}_{Q,l}$ according to (19)-(20) using only training symbols. Then the algorithm detects the data symbols based on the estimated weights. After that, these detected data symbols are used to refine the weights estimation, as additional training symbols. The updated weights are further used to demodulated the data symbols again. This goes back and forth till the symbol decisions will not change any more.

Removing the samples with small amplitude can greatly improve the reception performance without increasing implementation complexity, since monobit quantizer is sensitive to additive noise when the signal amplitude is small. The suboptimal monobit receiver for QPSK can employ this skill too, by setting the corresponding weights to zero. Different from the situation in BPSK, the samples either in the I or Q branch should be removed or not according the same threshold. Although the optimal threshold is hard to obtain, the performance is not sensitive to the threshold, which greatly increases the robustness of the receiver.

B. Performance Of Suboptimal Monobit Receiver

Similar to optimal monobit receiver in section III, we can calculate the bit error probability of the suboptimal receiver discussed above as follows

$$P_e = \sum_{\mathbf{r},\hat{\mathbf{w}}_I,\hat{\mathbf{w}}_Q} P_e\left(\mathbf{r},\hat{\mathbf{w}}_I,\hat{\mathbf{w}}_Q\right) P\left(\mathbf{r}\right) P\left(\hat{\mathbf{w}}_I,\hat{\mathbf{w}}_Q\right) \tag{21}$$

where $\hat{\mathbf{w}}_I = \left[\hat{w}_{I,0},...,\hat{w}_{I,N-1}\right]^T$ and $\hat{\mathbf{w}}_Q = \left[\hat{w}_{Q,0},...,\hat{w}_{Q,N-1}\right]^T$ are the estimated weights vectors. From (21), it can be observed that it is more complicated to calculate the error probability of the suboptimal receiver, compared with the one under optimal monobit receiver. Since the sum operation must be extended to cover all possible $\mathbf{r}$, $\hat{\mathbf{w}}_I$ and $\hat{\mathbf{w}}_Q$, which is prohibitive if N and N_t are relative large. Consequently, we evaluate the performance of the suboptimal monobit receiver under the performance criterion of deflection ratio.

From the estimation processes of the weights $\hat{w}_{I,l}$ and $\hat{w}_{Q,l}$ in (19) and (20), we can obtain

their mean values as follows

$$E\left\{\hat{w}_{I,l}\right\} = 1 - 2\epsilon_{I,l}, \quad E\left\{\hat{w}_{Q,l}\right\} = 1 - 2\epsilon_{Q,l} \tag{22}$$

The variances of $\hat{w}_{I,l}$ and $\hat{w}_{Q,l}$ are given as

$$Var\left\{\hat{w}_{I,l}\right\} = \frac{4\epsilon_{I,l}\left(1-\epsilon_{I,l}\right)}{N_t}, \quad Var\left\{\hat{w}_{Q,l}\right\} = \frac{4\epsilon_{Q,l}\left(1-\epsilon_{Q,l}\right)}{N_t} \tag{23}$$

With these knowledge, the deflection ratio of the suboptimal monobit receiver can be calculated as

$$D = \frac{\left[\sum_{l=0}^{N-1}\left(1-2\epsilon_{I,l}\right)^2 + \left(1-2\epsilon_{Q,l}\right)^2\right]^2}{\sum_{l=0}^{N-1}\left\{\left(1-2\epsilon_{I,l}\right)^2 + \left(1-2\epsilon_{Q,l}\right)^2 + 4\left[\epsilon_{I,l}\left(1-\epsilon_{I,l}\right) + \epsilon_{Q,l}\left(1-\epsilon_{Q,l}\right)\right]/N_t - 0.5\left[\left(1-2\epsilon_{I,l}\right)^2 + \left(1-2\epsilon_{Q,l}\right)^2\right]^2\right.} \tag{24}$$

We remark that the deflection ratio of the suboptimal receiver increases with the growth of the number of the training symbols, for a specific reference waveform $p_{ref}\left(t\right)$ and a specific phase difference φ.

When iterative demodulation is employed, the weights are updated during each iteration. To quantify the possible performance gain offered by the iteration demodulation, the deflection ratio after the nth iteration, denoted as D_n, is calculated. It turns out that D_n can be obtained by simply replacing N_t in (24) with $N_{t,n}^{eq}$, which can be regarded as the equivalent number of training symbols. Through some computation, we can derive $N_{t,n}^{eq}$ as follows

$$N_{t,n}^{eq} = \begin{cases} \frac{\left(N_t+N_d-N_{e,n-1}\right)^2}{N_t+N_d}, n \geq 1 \\ N_t, \qquad\qquad n = 0 \end{cases} \tag{25}$$

C. Effect Of Phase Difference

From (24), it can be observed that the deflection ratio only depends on $\epsilon_{I,l}$ and $\epsilon_{Q,l}$ when $N_{t,n}^{eq}$ is fixed. For a specific reference signal $p_{ref}\left(t\right)$, the parameters $\epsilon_{I,l}$ and $\epsilon_{Q,l}$ are only determined by the phase difference φ, which is constant but unknown to the receiver. As a result, the reception performance is affected by the phase difference.

The deflection ratios both in AWGN and fading channels, normalized by the maximum over $\varphi \in [0, \pi/2]$, are presented in Figure 2. It is observed that the deflection ratio will be bigger if the amplitudes of the I and Q branches are closer to each other, such as the situation when

$\varphi = \pi/4$. This leads to a better reception performance. Oppositely, the deflection ratio decreases significantly when the amplitude difference between the two branches is big, e.g. $\varphi = 0$, $\varphi = \pi/2$. Fortunately, the impact of the phase difference is much weaker in fading channel, thanks to the diversity offered by multipath. From this point of view, the suboptimal monobit receiver is benefited in fading channel.

D. Interface With Error-Control Decoder

Error-control coding is widely used in practical communication systems against noise and fading introduced by the channel. Some simple codes only employ binary demodulated data which is called ”hard” information for decoding. But some more powerful modern codes such as turbo, low-density parity-check (LDPC) or convolutional codes usually involve iterative decoding via a message passing algorithm [18], [19], [20]. Messages in the form of log-likelihood ratio (LLR), which is also called as ”soft” information, need to be fed to the decoder, as well as exchanged inside the decoder.

In the coded case of monobit receiver, the LLRs of the binary data d_{k0} and d_{k1} do not directly show up in the estimated log-likelihood functions presented in (18). However, through some approximations and processes in appendix A, the LLR of the data d_{k0} can be given as

$$\Lambda^{(opt)}\left(d_{k0}\right) = \log \frac{e^{\Lambda_k(d_{k1}=+1,d_{k0}=+1)} + e^{\Lambda_k(d_{k1}=-1,d_{k0}=+1)}}{e^{\Lambda_k(d_{k1}=+1,d_{k0}=-1)} + e^{\Lambda_k(d_{k1}=-1,d_{k0}=-1)}} \tag{26}$$

and we can also obtain the LLR of the data d_{k1} similarly as follows

$$\Lambda^{(opt)}\left(d_{k1}\right) = \log \frac{e^{\Lambda_k(d_{k1}=+1,d_{k0}=+1)} + e^{\Lambda_k(d_{k1}=+1,d_{k0}=-1)}}{e^{\Lambda_k(d_{k1}=-1,d_{k0}=+1)} + e^{\Lambda_k(d_{k1}=-1,d_{k0}=-1)}} \tag{27}$$

Substituting the symbol log-likelihood functions into (26) and (27), the LLR of the binary data can be obtained.

It can be observed that the calculation of the LLR employs exponent and logarithm operations. Both of them are usually realized by large lookup table in practical systems. As a result, search operation is also needed. All of these operations will introduce extremely high computation complexity.

To relax the computation requirement for (26) and (27), we can perform a Taylor’s expansion of the exponent and logarithm functions at 0 and 1 respectively, and obtain their first-order approximations. Thus, the suboptimal approximation of the LLR of data d_{k0} can be given as

$$\Lambda^{(sub)}\left(d_{k0}\right) = 2\left[\Lambda_k\left(d_{k1}=+1, d_{k0}=+1\right) - \Lambda_k\left(d_{k1}=+1, d_{k0}=-1\right)\right] \tag{28}$$

Analogously, the linear approximation of the LLR for data d_{k1} is given as follows

$$\Lambda^{(sub)}\left(d_{k1}\right)=2\left[\Lambda_k\left(d_{k1}=+1,d_{k0}=+1\right)-\Lambda_k\left(d_{k1}=-1,d_{k0}=+1\right)\right] \tag{29}$$

The details of the approximation process are presented in appendix A. We remark that these approximations may not be very accurate when $\Lambda_k\left(d_{k1},d_{k0}\right)$ is not very close to 0. This will lead to a performance degradation. Fortunately, as we will see in the numerical simulations, the performance degradation is slight and acceptable compared with the profits of the computation complexity reducing.

Substituting the estimated log-likelihood functions given by (18) into (28) and (29), the LLR of the binary data d_{k0} based on the training sequence under monobit sampling is given as

$$\tilde{\Lambda}^{(sub)}\left(d_{k0}\right)=2\sum_{l=0}^{N-1}\left[\left(\hat{w}_{I,l,n}+\hat{w}_{Q,l,n}\right)r_{I,k,l}-\left(\hat{w}_{I,l,n}-\hat{w}_{Q,l,n}\right)r_{Q,k,l}\right] \tag{30}$$

And similarly the LLR of d_{k1} is derived as follows

$$\tilde{\Lambda}^{(sub)}\left(d_{k1}\right)=2\sum_{l=0}^{N-1}\left[\left(\hat{w}_{I,l,n}-\hat{w}_{Q,l,n}\right)r_{I,k,l}+\left(\hat{w}_{I,l,n}+\hat{w}_{Q,l,n}\right)r_{Q,k,l}\right] \tag{31}$$

When the iteration demodulation is implemented, the weights are updated after every iteration based on the data sequence. Therein, it is extremely complex to calculate the precise LLR of the binary data. Define the decision statistic of the data d_{k0} as

$$\lambda\left(d_{k0}\right)=\sum_{l=0}^{N-1}\left[\left(w_{I,l,n}^{(iter)}+w_{Q,l,n}^{(iter)}\right)r_{I,k,l}-\left(w_{I,l,n}^{(iter)}-w_{Q,l,n}^{(iter)}\right)r_{Q,k,l}\right] \tag{32}$$

When N is relatively large, the decision statistic $\lambda\left(d_{k0}\right)$ can be treated as a Gaussian variable with mean $\bar{\lambda}_0$ and variance σ_0^2 conditioned on d_{k0}. Thus, we can scale the decision statistic by $2\bar{\lambda}_0/\sigma_0^2$ and used it as the LLR. The computation of $2\bar{\lambda}_0/\sigma_0^2$ from the monobit sampling result is given in [10]. Similarly, the decision statistic of data d_{k1} is obtained as follows

$$\lambda\left(d_{k1}\right)=\sum_{l=0}^{N-1}\left[\left(w_{I,l,n}^{(iter)}-w_{Q,l,n}^{(iter)}\right)r_{I,k,l}+\left(w_{I,l,n}^{(iter)}+w_{Q,l,n}^{(iter)}\right)r_{Q,k,l}\right] \tag{33}$$

Assuming that the mean and variance of $\lambda\left(d_{k1}\right)$ are $\bar{\lambda}_1$ and σ_1^2 respectively, then the scalar factor should been multiplied to $\lambda\left(d_{k1}\right)$ is $2\bar{\lambda}_1/\sigma_1^2$.

V. IQ IMBALANCE

IQ imbalance, caused by analog component imperfections, is a serious issue degrading the reception performance. However, it is unwise to compensate such impairment in the analog domain due to power and area costs. Therefore, economic schemes in the digital domain are desirable for wireless receivers. In this section, we first derive the formulation of the IQ imbalances similar to [15] for QPSK monobit receiver. Then problems of the application of the suboptimal monobit receiver presented in section IV with IQ imbalances are raised. Finally, the frame structure and the receiving method are modified to combat the performance degradation.

A. Formulation Of IQ Imbalances

The received baseband complex signal without IQ imbalance is given by (2) in section II. After being distorted by the IQ imbalance, the signal can be modeled as

$$r_d(t) = \mu r(t) + \upsilon r^*(t) \tag{34}$$

where μ and υ are parameters characterize the imbalances between the I and Q branches, including the amplitude imbalance and the phase imbalance. Let θ denote the phase deviation from the ideal 90° between the I and Q branches, and α denote the amplitude imbalance given as

$$\alpha = \frac{a_I - a_Q}{a_I + a_Q} \tag{35}$$

where a_I and a_Q are the gain amplitudes on the I and Q branches. When stated in dB, the amplitude imbalance is computed as $10\log(1+\alpha)$. The relations between μ, υ and θ, α are given as follows

$$\begin{aligned} \mu &= \cos(\theta/2) + j\alpha\sin(\theta/2) \\ \upsilon &= \alpha\cos(\theta/2) - j\sin(\theta/2) \end{aligned} \tag{36}$$

We remark that the receiver can not get access to the values of θ and α since they are caused by manufacturing inaccuracies in the analog components.

In order to get a more clear picture of the I and Q branch signals, we split the complex signal of (34) into the real and imaginary parts for a fixed symbol index k under the specific

transmitting constellation presented in section II as follows

$$r_d(t) = \begin{cases} (1+\alpha)\, p_{ref}(t)\cos(\varphi+\theta/2) + j*(1-\alpha)\, p_{ref}(t)\sin(\varphi-\theta/2) + n'(t), & d_1=1, d_0=1 \\ -(1+\alpha)\, p_{ref}(t)\sin(\varphi+\theta/2) + j*(1-\alpha)\, p_{ref}(t)\cos(\varphi-\theta/2) + n'(t), & d_1=1, d_0=-1 \\ (1+\alpha)\, p_{ref}(t)\sin(\varphi+\theta/2) - j*(1-\alpha)\, p_{ref}(t)\cos(\varphi-\theta/2) + n'(t), & d_1=-1, d_0=1 \\ -(1+\alpha)\, p_{ref}(t)\cos(\varphi+\theta/2) - j*(1-\alpha)\, p_{ref}(t)\sin(\varphi-\theta/2) + n'(t), & d_1=-1, d_0=-1 \end{cases} \tag{37}$$

where the symbol index k and its corresponding delay kT_s are suppressed to simplify the notation. The average amplitude of the I and Q branches is assumed to be unity. Compared with (7), it can be observed that the useful signal of the I branch of the symbol $(d_1=1, d_0=1)$ is no longer the same as the one of the Q branch of the symbol $(d_1=1, d_0=-1)$. In fact, it is this difference that greatly affects the reception performance.

In the next subsections, we will first discuss the effect of the IQ imbalances based on the formulation above. Then, the frame structure and the suboptimal monobit receiver proposed before are modified to adapt to the communication environment with IQ imbalances.

B. Effect of IQ Imbalances

In (37), we notice that when $\alpha = 0$ and $\theta = 0$, that means there is no IQ imbalance at the receiver, (37) degrades to (7) and we have the following relations as

$$\begin{aligned} r_{d,I}(t|d_1=1, d_0=1) &= r_{d,Q}(t|d_1=1, d_0=-1) \\ r_{d,Q}(t|d_1=1, d_0=1) &= -r_{d,I}(t|d_1=1, d_0=-1) \end{aligned} \tag{38}$$

where $r_{d,I}(t|d_1, d_0)$ denotes the useful signal of the I branch when the symbol (d_1, d_0) is transmitted, and $r_{d,Q}(t|d_1, d_0)$ denotes the corresponding useful signal of the Q branch. In this case, transmitting the symbol $(1, 1)$ for training is quite enough to demodulate the data by employing the suboptimal monobit receiver presented in (18). We remark that the relations given in (38) are the bases of the suboptimal monobit receiver.

However, the equations in (38) can not be held when the IQ imbalances exist at the receiver. If $\alpha \neq 0$, $\theta = 0$, which means there is only amplitude imbalance at the receiver, then $r_{d,I}(t|d_1=1, d_0=1)$ and $r_{d,Q}(t|d_1=1, d_0=-1)$ will certainly have different amplitudes, but the same sign as the situation without the IQ imbalance. Similarly, $r_{d,Q}(t|d_1=1, d_0=1)$ and

$r_{d,I}\left(t|d_1=1,d_0=-1\right)$ will still have opposite signs even with different amplitudes. In this case, using the suboptimal monobit receiver for detection will certainly suffer a performance degradation. Fortunately, this kind of performance degradation is acceptable as we will see in the numerical simulations, thanks to the 1-bit sampling's insensitiveness to the amplitude.

When there is phase imbalance at the receiver, the situation becomes more severe. $r_{d,I}\left(t|d_1=1,d_0=1\right)$ and $r_{d,Q}\left(t|d_1=1,d_0=-1\right)$ will certainly have different amplitudes. However, they may have the same sign or not, depending on the phase difference φ and the phase imbalance parameter θ. On the other hand, the relation between $r_{d,Q}\left(t|d_1=1,d_0=1\right)$ and $r_{d,I}\left(t|d_1=1,d_0=-1\right)$ is similar except that they should have the opposite sign without the phase imbalance. If the relations of the two "couples" about the sign can be satisfied under the IQ imbalances (e.g. $\varphi=\pi/4$, $\theta=5^\circ$), the suboptimal receiver can still work at the price of some performance loss. Otherwise, the reception performance degrades severely. For example, the suboptimal receiver will confuse the symbol $(d_1=1,d_0=1)$ with the symbol $(d_1=1,d_0=-1)$ or $(d_1=-1,d_0=1)$ with high probability when $\varphi=0$, $\theta=5^\circ$, where the sign relations can not be held. Hence, a monobit receiver maintaining better performance under these conditions is desirable.

C. Suboptimal Monobit Receiver Based On Double Training Sequences

To combat the reception performance loss introduced by the IQ imbalances, a strategy using double training sequences is employed. The first training sequence consists of $N_t^{(0)}$ symbols of $(d_1=1,d_0=1)$. The second training sequence consists of $N_t^{(1)}$ symbols of $(d_1=1,d_0=-1)$. Let $N_t=N_t^{(0)}+N_t^{(1)}$ to maintain the efficiency of the system. Usually, we have $N_t^{(0)}=N_t^{(1)}=N_t/2$.

Based on the first training sequence, we can obtain the ML estimation of the weight of the I branch $\hat{w}_{I,l}^{(0)}$ as follows

$$\hat{w}_{I,l}^{(0)}=\frac{1}{N_t^{(0)}}\sum_{k=0}^{N_t^{(0)}-1}r_{I,k,l},\quad 0\le l<N-1 \tag{39}$$

Similarly, the estimated weight associated with the Q branch, denoted as $\hat{w}_{Q,l}^{(0)}$, is given by

$$\hat{w}_{Q,l}^{(0)}=\frac{1}{N_t^{(0)}}\sum_{k=0}^{N_t^{(0)}-1}r_{Q,k,l},\quad 0\le l<N-1 \tag{40}$$

Based on the second training sequence, we can similarly obtain the ML estimations of the weights of the I and Q branches as follows

$$\hat{w}_{I,l}^{(1)} = \frac{1}{N_t^{(1)}} \sum_{k=0}^{N_t^{(1)}-1} r_{I,k,l}, \quad 0 \le l < N-1 \tag{41}$$

$$\hat{w}_{Q,l}^{(1)} = \frac{1}{N_t^{(1)}} \sum_{k=0}^{N_t^{(1)}-1} r_{Q,k,l}, \quad 0 \le l < N-1 \tag{42}$$

We can directly replace the estimated weights $\hat{w}_{I,l}$, $\hat{w}_{Q,l}$ in the suboptimal monobit receiver with $\hat{w}_{I,l}^{(0)}$, $\hat{w}_{Q,l}^{(0)}$, $\hat{w}_{I,l}^{(1)}$ and $\hat{w}_{Q,l}^{(1)}$ which are estimated through the double training sequences. Then we can derive the linear approximations of the log-likelihood functions based on the double training sequences as follows

$$\begin{aligned}
\Lambda_k^{(dt)}\left(d_{k1}=1, d_{k0}=1\right) &= \sum_{l=0}^{N-1} \hat{w}_{I,l}^{(0)} r_{I,k,l} + \hat{w}_{Q,l}^{(0)} r_{Q,k,l} \\
\Lambda_k^{(dt)}\left(d_{k1}=1, d_{k0}=-1\right) &= \sum_{l=0}^{N-1} \hat{w}_{I,l}^{(1)} r_{I,k,l} + \hat{w}_{Q,l}^{(1)} r_{Q,k,l} \\
\Lambda_k^{(dt)}\left(d_{k1}=-1, d_{k0}=1\right) &= -\sum_{l=0}^{N-1} \hat{w}_{I,l}^{(1)} r_{I,k,l} - \hat{w}_{Q,l}^{(1)} r_{Q,k,l} \\
\Lambda_k^{(dt)}\left(d_{k1}=-1, d_{k0}=-1\right) &= -\sum_{l=0}^{N-1} \hat{w}_{I,l}^{(0)} r_{I,k,l} - \hat{w}_{Q,l}^{(0)} r_{Q,k,l}
\end{aligned} \tag{43}$$

After acquiring the log-likelihood functions, the suboptimal monobit receiver based on the double training sequences is given in (13), by replacing $\Lambda_k^{(opt)}\left(d_{k1}, d_{k0}\right)$ with $\Lambda_k^{(dt)}\left(d_{k1}, d_{k0}\right)$.

To evaluate the performance of the monobit receiver proposed above, the deflection ratio of such receiver is calculated in the following. First of all, define

$$\begin{aligned}
\epsilon_{I,l}^{(0)} &= Q\left(r_{d,I}\left(lT|d_1=1, d_0=1\right)\right), \quad \epsilon_{Q,l}^{(0)} = Q\left(r_{d,Q}\left(lT|d_1=1, d_0=1\right)\right) \\
\epsilon_{I,l}^{(1)} &= Q\left(r_{d,I}\left(lT|d_1=1, d_0=-1\right)\right), \quad \epsilon_{Q,l}^{(1)} = Q\left(r_{d,Q}\left(lT|d_1=1, d_0=-1\right)\right)
\end{aligned} \tag{44}$$

The means and variances of the weights in (39)-(42) can be calculated similarly in the way of the practical monobit receiver based on single training sequence. Then, we redefine the decision statistic as $\lambda^{(dt)} = \Lambda^{(dt)}\left(d_1=1, d_0=1\right)$. Through some computation, the deflection ratio of the suboptimal monobit receiver in (43) is given as follows

$$D^{(dt)} = \frac{4\left[\sum_{l=0}^{N-1}\left(1-2\epsilon_{I,l}^{(0)}\right)\left(\epsilon_{I,l}^{(1)}-\epsilon_{I,l}^{(0)}\right)+\left(1-2\epsilon_{Q,l}^{(0)}\right)\left(\epsilon_{Q,l}^{(1)}-\epsilon_{Q,l}^{(0)}\right)\right]^2}{Var\left(\lambda^{(dt)}\right)} \tag{45}$$

where $Var\left(\lambda^{(dt)}\right)$ is given as follows

$$\begin{aligned} Var\left(\lambda^{(dt)}\right) = & \sum_{l=0}^{N-1} 4\left[\epsilon_{I,l}^{(0)}\left(1-\epsilon_{I,l}^{(0)}\right)+\epsilon_{Q,l}^{(0)}\left(1-\epsilon_{Q,l}^{(0)}\right)\right]/N_t^{(0)} + \left(1-2\epsilon_{I,l}^{(0)}\right)^2 + \left(1-2\epsilon_{Q,l}^{(0)}\right)^2 \\ & - 0.5\left[\left(1-2\epsilon_{I,l}^{(0)}\right)^2\left(\left(1-2\epsilon_{I,l}^{(0)}\right)^2+\left(1-2\epsilon_{I,l}^{(1)}\right)^2\right)\right] \\ & - 0.5\left[\left(1-2\epsilon_{Q,l}^{(0)}\right)^2\left(\left(1-2\epsilon_{Q,l}^{(0)}\right)^2+\left(1-2\epsilon_{Q,l}^{(1)}\right)^2\right)\right] \end{aligned} \tag{46}$$

From (45), it can be observed that the monobit receiver based on double training sequences can outperform the receiver in (18) when the sign relations of the two "couples" can not be satisfied. Besides, the reception performance will be improved as the length of the first training sequence increases, which is just the half of the single training sequence to maintain the communication efficiency. From this point of view, we can increase the performance if we increase the equivalent number of the training sequences. This leads to a improved monobit receiver based on double training sequences.

D. Monobit Receiver With Combinational Weights

In a practical system, the amplitude imbalance α is usually less than 0.1 and the phase deviation θ is usually less than $2.5°$. Consequently, the amplitude difference caused by the amplitude and phase imbalances is limited. Considering 1-bit sampling is insensitive to the amplitude, it is reasonable to assume that $r_{d,Q}\left(t|d_1=1,d_0=-1\right) \approx A r_{d,I}\left(t|d_1=1,d_0=1\right)$ and $r_{d,I}\left(t|d_1=1,d_0=-1\right) \approx B r_{d,Q}\left(t|d_1=1,d_0=1\right)$ by ignoring the amplitude difference. The A and B are called sign factors here, which are determined by the phase imbalance θ and the phase difference φ. A is asserted to be 1 when $r_{d,I}\left(t|d_1=1,d_0=1\right)$ and $r_{d,Q}\left(t|d_1=1,d_0=-1\right)$ have the same sign, or else $A=-1$. On the other hand, the value of B is chosen analogously to A.

To make use of the double training sequences more sophisticatedly, the weights estimated using (39)-(42) are combined in the following way to reduce the variances. The combinational weights are given as follows

$$\hat{w}_{I,l}^{(cw)} = \frac{1}{2}\hat{w}_{I,l}^{(0)} + \frac{\hat{A}}{2}\hat{w}_{Q,l}^{(1)} \tag{47}$$

$$\hat{w}_{Q,l}^{(cw)} = \frac{1}{2}\hat{w}_{Q,l}^{(0)} + \frac{\hat{B}}{2}\hat{w}_{I,l}^{(1)} \tag{48}$$

where $\hat{A}$ and $\hat{B}$ are the estimations of the sign factor A and B respectively, which are not known to the receiver due to the absence of the precise θ and φ. The estimation process is realized through the training sequences. Certainly, we can obtain the ML estimations of the sign factors. However, the computation complexity of such estimation is extremely high. Consequently, a simple but effective method is proposed to estimate the sign factor A as follows

$$\hat{A} = \mathrm{sgn}\left(\sum_{l=0}^{N-1} \hat{w}_{I,l}^{(0)} \hat{w}_{Q,l}^{(1)}\right) \tag{49}$$

It is interesting that the estimator appears in the form of a correlator. Similarly, the sign factor B is estimated by

$$\hat{B} = \mathrm{sgn}\left(\sum_{l=0}^{N-1} \hat{w}_{Q,l}^{(0)} \hat{w}_{I,l}^{(1)}\right) \tag{50}$$

After obtaining the estimations of the sign factors, the combinational weights $\hat{w}_{I,l}^{(cw)}$ and $\hat{w}_{Q,l}^{(cw)}$ can be simply calculated using (47) and (48) respectively. Then the monobit receiver with combinational weights based on the double training sequences is derived as follows

$$\begin{aligned}
\Lambda_k^{(cw)}\left(d_{k1}=1, d_{k0}=1\right) &= \sum_{l=0}^{N-1} \hat{w}_{I,l}^{(cw)} r_{I,k,l} + \hat{w}_{Q,l}^{(cw)} r_{Q,k,l} \\
\Lambda_k^{(cw)}\left(d_{k1}=1, d_{k0}=-1\right) &= \sum_{l=0}^{N-1} \hat{B}\hat{w}_{Q,l}^{(cw)} r_{I,k,l} + \hat{A}\hat{w}_{I,l}^{(cw)} r_{Q,k,l} \\
\Lambda_k^{(cw)}\left(d_{k1}=-1, d_{k0}=1\right) &= -\sum_{l=0}^{N-1} \hat{B}\hat{w}_{Q,l}^{(cw)} r_{I,k,l} - \hat{A}\hat{w}_{I,l}^{(cw)} r_{Q,k,l} \\
\Lambda_k^{(cw)}\left(d_{k1}=-1, d_{k0}=-1\right) &= -\sum_{l=0}^{N-1} \hat{w}_{I,l}^{(cw)} r_{I,k,l} - \hat{w}_{Q,l}^{(cw)} r_{Q,k,l}
\end{aligned} \tag{51}$$

The performance of the monobit receiver with combinational weights measured in the deflection ratio is calculated in appendix B. When $A=1$ and $B=-1$, we can assume that $\epsilon_{I,l}^{(0)} \approx \epsilon_{Q,l}^{(1)}$ and $\epsilon_{Q,l}^{(0)} \approx 1-\epsilon_{I,l}^{(1)}$. Under this condition, we can obtain $D^{(cw)} > D^{(dt)}$. Therefore, the monobit receiver with combinational weights do increase the reception performance. And this will be proved in the numerical results.

E. Dithering

The Gaussian-shaped or raised cosine pulse is widely used for wide band communication. They both have a main lobe and two relative small side-lobes. Unfortunately, the main lobes of

two branches may have the same sampling results in the intermediate SNR region, when phase difference φ is around 0 or $\pi/2$ and IQ imbalances exist. In this case, the side-lobes become the determinant factor and the BER increases. Thanks to the diversity offered by the multi-paths, this won't be a issue in fading channel.

To combat such performance degradation, Gaussian dithering to ADC input is efficient. Other methods including automatic gain control at the receiver or power control at the transmitter are feasible two. All of them need to estimate the rough region of the SNR. This can be simply implemented by counting the number of weights that equals to 1.

VI. Application To Ultra-Wideband Signaling And Numerical Results

A. Application To Ultra-wideband Signaling

The receivers obtained in this paper are particularly suitable to processing ultra-wideband signals. The main reason is that the Nyquist sampling rates of such UWB signals are up to multi giga hertz. At such high rate, high-precision ADC is extremely costly and power-hungry to implement. Consequently, one bit receiver is a wise choice for ultra-wideband processing.

In general UWB communication system, a raised cosine pulse is used, which is given as

$$p_{tr}(t) = \operatorname{sinc}(t/\tau) \frac{\cos(\pi\beta t/\tau)}{1 - 4\beta^2 t^2/\tau^2} \tag{52}$$

where τ is the time constant that controls the pulse duration, and β is the roll-off factor.

In the following, simulation results are provided to evaluate the performance of the monobit receivers proposed in this paper in UWB environment. The raised cosine pulse was adopted with $\tau = 0.5ns$ and $\beta = 1$. The bandwidth of the low-pass filter was B = 5GHz, and the sampling rate was Nyquist rate T = 100ps. We assume that there is no ISI and the timing is perfect. The number of data symbols was $N_d = 1000$, and the length of the training sequence was $N_t = 100$. The training overhead amounts to 10 per cent of the total transmission duration. The SNR is defined as $E_b/N_0 = \sum_{l=1}^{N} p_{ref}^2(lT)$. For the simulations in multipath fading channel, we used the standard CM1 channel model with 100 realizations [21].

B. Receiver Considered

To simplify the notation in the next discussion, we use abbreviations. The first part of the abbreviation is either FR or MB, indicating whether full-resolution ADC or monobit sampling is

used. The second part is either E or F indicating whether estimated or full CSI is used in obtaining the weighting signal for detection. The third part is one of ML, MF, TE, RV, or IR, indicating the type of weighting method used, corresponding to the optimal weights in (12), the matched-filter weights, the suboptimal weights in (18) obtained from Taylor's expansion. For the simulations with the IQ imbalances, the abbreviations DT and CW indicate the weights in (39)-(42) and the combinational weights in (47)-(48) respectively, based on the double training sequences. Finally, the suffix RV indicates the receiver removes the samples with small amplitude, IR represents that the iteration demodulation is employed with removing small samples, and SI indicates the sign factors are available at the receiver.

Use such notation, the receivers that we will consider are as follows:

1) FR-F-MF: the optimal receiver with full-resolution sampling, full CSI, and matched-filter weights.

2) MB-F-ML: the optimal receiver with monobit sampling, full CSI, and optimal weights in (12).

3) MB-F-MF: the monobit receiver with full CSI and the matched filter weights.

4) MB-E-TE: the monobit receiver with estimated CSI, Taylor's expansion approximated weights.

5) MB-E-TE-RV: MB-E-TE receiver with removal of small samples.

6) MB-E-TE-IR: MB-E-RV receiver with demodulation iteration.

7) MB-E-MF-SI: the monobit receiver with full CSI, the sign factor information, and matched filter weights.

8) MB-E-DT: the monobit receiver with estimated CSI, Taylor's expansion approximated weights based on double training sequences.

9) MB-E-DT-IR: MB-E-DT receiver with iteration and removal of small samples.

10) MB-E-CW: the monobit receiver with estimated CSI, combinational weights based on double training.

11) MB-E-CW-IR: MB-E-CW receiver with iteration and removal of small samples.

C. Numerical Results

Figure. 3 compares the performance of different receivers in AWGN channel without IQ imbalances. Given the perfect reference signal (which is not possible in practice though), the

MB-F-MF and MB-F-ML receivers have similar performance in entire SNR range. Both of them have about 5dB SNR loss to the full-resolution matched filter when the BER is around 10^{-3}. The threshold $A_{th}^{(r)}$ of the MB-E-TE-RV receiver is 0.2. The number of the iterations we use here is 4. We observe that the MB-E-TE-RV receiver can provide about 2dB performance gain compared with the MB-E-TE receiver, without increasing too much complexity. The MB-E-TE-IR receiver can offer another 1dB performance gain. Thus, it only has about 3dB performance degradation to the monobit receiver with full CSI.

The performance under fading channel is shown in Figure. 4. Similarly to the AWGN channel, the MB-F-MF and MB-F-ML receiver have almost the same performance in fading channel. The gap between them and the FR-F-MF receiver has decreased to 2dB. The MB-E-TE-IR receiver still outperforms the MB-E-TE receiver about 3dB performance gain. Besides, the gap between the MB-F-ML and MB-E-TE-IR has been narrowed to 1dB. Unfortunately, the gain offered by removal of small samples is diminished.

Figure. 5 shows the effect of the phase difference on the practical monobit receiver in AWGN channel without IQ imbalances. The number suffixed to the abbreviations of the receivers indicates the degree of the phase difference, e.g. $\varphi = 0^{\circ}$. It can be observed that the MB-E-TE-IR receiver is greatly affected by the phase difference. The reception performance is much better when the amplitudes of the I and Q branches are close to each other ($\varphi = 45^{\circ}$), which is consistent with the calculation result of the deflection ratio in Figure. 2. The performance of the MB-E-TE-IR receiver under different φ in fading channel is presented in Figure. 6, which shows that the effect of the phase different on fading channel is weak, thanks to the diversity offed by the multipath.

Figure. 7 presents the performance of the MB-E-TE receiver under the error-control coding without IQ imbalances. The error-control code used here is convolutional code with 1/2 rate. The abbreviation MB-E-TE here indicates the BER in uncoded setup. The notation ”Hard” represents the performance of feeding the hard decision to the decoder. ”Soft-Opt” corresponds to feed the LLR in (26) and (27) to the decoder, and ”Soft-Sub” indicates the LLRs in (28) and (29) are fed to the decoder. We can observe that the ”Soft-Sub” performs as well as the ”Soft-Opt”, and both of them have a 3dB performance gain compared with the hard decoding.

In Figure. 8, we illustrate the impact of the amplitude imbalance on the practical monobit receiver. The number suffixed to the abbreviations represents the value of the amplitude imbalance.

We observe that the performance degradation caused by the amplitude imbalance is negligible when $\alpha = 0.1$. And there is only about 1dB performance loss when $\alpha = 0.2$. Thus, it is fair enough to claim that it is not the amplitude imbalance that dramatically degrade the reception performance.

Figure. 9 gives the performance of different receivers in AWGN channel with IQ imbalances. The amplitude imbalance $\alpha = 0.1$ and the phase imbalance $\theta = 2.5^\circ$. When the double training sequences are used, we let $N_t^{(0)} = N_t^{(1)} = N_t/2 = 50$ to maintain system efficiency. It shows that even the matched-filter receiver without the information of the sign factors has a 10^{-2} error floor at the high SNR region, the same as the MB-E-TE-IR receiver. The main reason of this error floor is the sign relations in (38) can not be held, which makes a lot of confusion for the receiver. With the knowledge of the sign factors, the MB-F-MF-SI receiver has a BER increasing when the SNR is in 25-40dB. This is mainly caused by the side-lobes of the pulse and the IQ imbalances. The performance of the MB-E-DT-IR and MB-E-CW-IR receivers are more smoothly. Both of them have only about 1dB performance loss at high SNR region compared with the MB-F-MF-SI receiver. Besides, the MB-E-CW-IR receiver outperforms MB-E-DT-IR receiver as analyzed before. The simulation results here also prove the importance of estimating the sign factors in AWGN channel.

Figure. 10 presents the performance of different receivers with IQ imbalances in fading channel. The parameters of the IQ imbalance are the same as the ones in AWGN channel. Thanks to the diversity offered by the multipath, all receivers have almost no performance loss compared with the performance without IQ imbalances in Figure. 4, except for the MB-E-DT and MB-E-DT-IR receivers whose performance is limited by the equivalent number of the training sequence. The MB-E-CW receiver slightly outperforms the MB-E-TE receiver, and the MB-E-CW-IR and MB-E-TE-IR receivers have the same performance. It can been observed that the effect of the IQ imbalance at the receiver in fading channel is negligible.

VII. Conclusions

We have derived the optimal ML receiver with monobit sampling for QPSK modulation and its corresponding performance in the form of the deflection ratio. To reduce the implementation complexity, we extend the main idea of [10] to the optimal monobit receiver, and obtain a linear suboptimal monobit receiver for QPSK modulation. The iteration demodulation and removal of

small samples are modified to suit for QPSK too. We investigate the effect of the phase difference between the transmitter and the receiver. And the LLR of the binary data fed to error-control decoder is derived from the log-likelihood functions of the QPSK symbols. We simulated the practical monobit receiver in the UWB communication system. We showed that such monobit greatly reduce the complexity at the price of about 3dB SNR loss in AWGN channel and 1dB SNR loss in fading channel, compared with the matched filter based monobit receiver with full CSI. We also observe that the reception performance will be better if the amplitudes of the two branches are close to each other.

We have investigated the effect of the IQ imbalances at the receiver. To combat the performance loss introduced by the IQ imbalances, two receiver based on the double training sequences have been proposed. Simulation results showed that the impact of the amplitude imbalance is weak. We noticed that the proposed monobit receiver can efficiently compensate the SNR loss in AWGN channel, especially when SNR is high. The performance loss of all these receivers in fading channel is acceptable, thanks to the diversity offered by the multipath.

Due to the economic efficiency and technical simplicity, the digital receivers with monobit sampling are strongly candidates for future communication systems with significantly large bandwidth, such as UWB communication or communication in 60G band. There are several open issues to be addressed, such as evaluating the performance of the monobit receiver under QAM modulation, or in frequency asynchronous system.

APPENDIX A

In this appendix, we first derive the LLRs of the binary data d_{k0} and d_{k1} based on the estimated log-likelihood functions in (18). Next, we obtain a linear approximation of the LLR through Taylor expansion, to reduce the computational complexity.

The log-likelihood function $\Lambda_k^{(opt)}(d_{k1}, d_{k0})$ of each received QPSK symbol is given by (12) in section III. Via Taylor expansion of the logarithm in $\Lambda_k^{(opt)}(d_{k1}, d_{k0})$ and discarding the constant $-2N\log 2$, we obtain the approximate estimated log-likelihood functions $\Lambda_k(d_{k1}, d_{k0})$ presented in (18). Thus, we can derive the relation between $\Lambda_k^{(opt)}(d_{k1}, d_{k0})$ and $\Lambda_k(d_{k1}, d_{k0})$ as follows

$$\Lambda_k^{(opt)}(d_{k1}, d_{k0}) \approx \Lambda_k(d_{k1}, d_{k0}) - 2N\log 2 \tag{53}$$

Note that $\Lambda_k^{(opt)}(d_{k1}, d_{k0}) = \log P(\mathbf{r}_k|d_{k1}, d_{k0})$, we arrive at

$$P(\mathbf{r}_k|d_{k1}, d_{k0}) \approx e^{\Lambda_k(d_{k1},d_{k0})-2N\log 2} \tag{54}$$

According to probability theories, it is clear that

$$\begin{aligned} P(\mathbf{r}_k|d_{k0}=+1) = {} & P(d_{k1}=+1)\, P(\mathbf{r}_k|d_{k1}=+1, d_{k0}=+1) \\ & + P(d_{k1}=-1)\, P(\mathbf{r}_k|d_{k1}=-1, d_{k0}=+1) \end{aligned} \tag{55}$$

$$\begin{aligned} P(\mathbf{r}_k|d_{k0}=-1) = {} & P(d_{k1}=+1)\, P(\mathbf{r}_k|d_{k1}=+1, d_{k0}=-1) \\ & + P(d_{k1}=-1)\, P(\mathbf{r}_k|d_{k1}=-1, d_{k0}=-1) \end{aligned} \tag{56}$$

In practice, we usually have $P(d_{k1}=+1) = P(d_{k1}=-1) = 1/2$. Considering data d_{k0} and d_{k1} are independent to each other, the LLR of the data d_{k0} is given as follows

$$\Lambda^{(opt)}(d_{k0}) = \log \frac{P(\mathbf{r}_k|d_{k1}=+1, d_{k0}=+1) + P(\mathbf{r}_k|d_{k1}=-1, d_{k0}=+1)}{P(\mathbf{r}_k|d_{k1}=+1, d_{k0}=-1) + P(\mathbf{r}_k|d_{k1}=-1, d_{k0}=-1)} \tag{57}$$

Substituting (54) into (57) and eliminating the common factor $e^{-2N\log 2}$ in the numerator and denominator, we can obtain the optimal LLR of the data d_{k0} as follows

$$\Lambda^{(opt)}(d_{k0}) = \log \frac{e^{\Lambda_k(d_{k1}=+1,d_{k0}=+1)} + e^{\Lambda_k(d_{k1}=-1,d_{k0}=+1)}}{e^{\Lambda_k(d_{k1}=+1,d_{k0}=-1)} + e^{\Lambda_k(d_{k1}=-1,d_{k0}=-1)}} \tag{58}$$

Analogously, the optimal LLR of the binary data d_{k1} is given by

$$\Lambda^{(opt)}(d_{k1}) = \log \frac{e^{\Lambda_k(d_{k1}=+1,d_{k0}=+1)} + e^{\Lambda_k(d_{k1}=+1,d_{k0}=-1)}}{e^{\Lambda_k(d_{k1}=-1,d_{k0}=+1)} + e^{\Lambda_k(d_{k1}=-1,d_{k0}=-1)}} \tag{59}$$

In order to reduce the computational complexity of the LLR of the binary data, which is mainly caused by the exponent and logarithm operations in (58) and (59), we can perform a Taylor's expansion of the exponent and logarithm functions and obtain a first-order linear approximation of the LLR. From (18), we note that $\Lambda_k(d_{k1}=1, d_{k0}=1) = -\Lambda_k(d_{k1}=-1, d_{k0}=-1)$ and $\Lambda_k(d_{k1}=1, d_{k0}=-1) = -\Lambda_k(d_{k1}=-1, d_{k0}=1)$. Therefore, it is reasonable to assume that $\Lambda_k(d_{k1}, d_{k0})$ is symmetrically distributed around zero. Then the first order approximation of the exponent function of $\Lambda_k(d_{k1}, d_{k0})$ around zero is given by

$$e^{\Lambda_k(d_{k1},d_{k0})} \approx 1 + \Lambda_k(d_{k1}, d_{k0}) \tag{60}$$

On the other hand, we have the first-order approximation of the logarithm function around 1 as $\log(1+x) \approx x$. Then it is straightforward to derive the suboptimal approximate LLR of the

data d_{k0} as

$$\begin{aligned}\Lambda^{(sub)}(d_{k0}) &= \frac{\log\left(2+\Lambda_k(d_{k1}=1,d_{k0}=1)+\Lambda_k(d_{k1}=-1,d_{k0}=1)\right)}{\log\left(2+\Lambda_k(d_{k1}=1,d_{k0}=-1)+\Lambda_k(d_{k1}=-1,d_{k0}=-1)\right)} \\ &= \Lambda_k(d_{k1}=1,d_{k0}=1)+\Lambda_k(d_{k1}=-1,d_{k0}=1) \\ &\quad -\Lambda_k(d_{k1}=1,d_{k0}=-1)-\Lambda_k(d_{k1}=-1,d_{k0}=-1) \\ &= 2\left[\Lambda_k(d_{k1}=1,d_{k0}=1)-\Lambda_k(d_{k1}=1,d_{k0}=-1)\right] \end{aligned} \tag{61}$$

Similarly, the suboptimal approximate LLR of the data d_{k1} is given by

$$\Lambda^{(sub)}(d_{k1}) = 2\left[\Lambda_k(d_{k1}=+1,d_{k0}=+1)-\Lambda_k(d_{k1}=-1,d_{k0}=1)\right] \tag{62}$$

APPENDIX B

In this section, we calculate the deflection ratio of the monobit receiver with combinational weights based on the double training sequences in (51). To simplify the computation process, we assume that the sign factors have been estimated correctly.

At the beginning, the decision statistic is defined as $\lambda = \Lambda_k^{(cw)}(d_{k1}=1,d_{k0}=1)$. Although both the sign factors and the combinational weights are estimated from the samples of the training sequences, we assume that they are independent to each other for simplicity of analysis. In fact, the dependency between them is small if the number N of samples per symbol is large. Then the means of the combinational weights in (47) and (48) are given as follows

$$\begin{aligned} E\left\{\hat{w}_{I,l}^{(cw)}\right\} &= \frac{1}{2}\left(1-2\epsilon_{I,l}^{(0)}\right)+\frac{A}{2}\left(1-2\epsilon_{Q,l}^{(1)}\right) \\ E\left\{\hat{w}_{Q,l}^{(cw)}\right\} &= \frac{1}{2}\left(1-2\epsilon_{Q,l}^{(0)}\right)+\frac{B}{2}\left(1-2\epsilon_{I,l}^{(1)}\right) \end{aligned} \tag{63}$$

and the variances of the weights are given as

$$\begin{aligned} Var\left\{\hat{w}_{I,l}^{(cw)}\right\} &= \frac{\epsilon_{I,l}^{(0)}\left(1-\epsilon_{I,l}^{(0)}\right)}{N_t^{(0)}}+\frac{\epsilon_{Q,l}^{(1)}\left(1-\epsilon_{Q,l}^{(1)}\right)}{N_t^{(1)}} \\ Var\left\{\hat{w}_{Q,l}^{(cw)}\right\} &= \frac{\epsilon_{Q,l}^{(0)}\left(1-\epsilon_{Q,l}^{(0)}\right)}{N_t^{(0)}}+\frac{\epsilon_{I,l}^{(1)}\left(1-\epsilon_{I,l}^{(1)}\right)}{N_t^{(1)}} \end{aligned} \tag{64}$$

After obtaining the means and variances of the weights, we can directly calculate the deflection ratio of the monobit receiver in (51). Let $D^{(cw)} = D_{num}^{(cw)}/D_{den}^{(cw)}$ denote the deflection ration. Then

the numerator and denominator are given as follows

$$\begin{aligned} D_{num}^{(cw)} &= \left(1-2\epsilon_{I,l}^{(0)}\right)^2 + \left(1-2\epsilon_{Q,l}^{(0)}\right)^2 + (A+B)\left(1-2\epsilon_{I,l}^{(1)}\right)\left(1-2\epsilon_{Q,l}^{(1)}\right) \\ &+ A\left(1-2\epsilon_{I,l}^{(0)}\right)\left(1-2\epsilon_{Q,l}^{(1)}\right) + B\left(1-2\epsilon_{I,l}^{(1)}\right)\left(1-2\epsilon_{Q,l}^{(0)}\right) \\ &+ \left(1-2\epsilon_{I,l}^{(0)}\right)\left(1-2\epsilon_{I,l}^{(1)}\right) + \left(1-2\epsilon_{Q,l}^{(0)}\right)\left(1-2\epsilon_{Q,l}^{(1)}\right) \end{aligned} \tag{65}$$

$$\begin{aligned} D_{den}^{(cw)} &= \left[\epsilon_{I,l}^{(0)}\left(1-\epsilon_{I,l}^{(0)}\right) + \epsilon_{Q,l}^{(0)}\left(1-\epsilon_{Q,l}^{(0)}\right)\right]/N_t^{(0)} + \left[\epsilon_{I,l}^{(1)}\left(1-\epsilon_{I,l}^{(1)}\right) + \epsilon_{Q,l}^{(1)}\left(1-\epsilon_{Q,l}^{(1)}\right)\right]/N_t^{(1)} \\ &+ 0.5\left[\left(1-2\epsilon_{I,l}^{(0)}\right) + A\left(1-2\epsilon_{Q,l}^{(1)}\right)\right]^2\left[\epsilon_{I,l}^{(0)}\left(1-\epsilon_{I,l}^{(0)}\right) + \epsilon_{I,l}^{(1)}\left(1-\epsilon_{I,l}^{(1)}\right)\right] \\ &+ 0.5\left[\left(1-2\epsilon_{Q,l}^{(0)}\right) + B\left(1-2\epsilon_{I,l}^{(1)}\right)\right]^2\left[\epsilon_{Q,l}^{(0)}\left(1-\epsilon_{Q,l}^{(0)}\right) + \epsilon_{Q,l}^{(1)}\left(1-\epsilon_{Q,l}^{(1)}\right)\right] \end{aligned} \tag{66}$$

REFERENCES

[1] P. Smulders, "Exploiting the 60 ghz band for local wireless multimedia access: prospects and future directions," *Communications Magazine, IEEE*, vol. 40, no. 1, pp. 140 –147, jan 2002.

[2] Y. Chiu, B. Nikolic, and P. Gray, "Scaling of analog-to-digital converters into ultra-deep-submicron cmos," in *Custom Integrated Circuits Conference, 2005. Proceedings of the IEEE 2005*, sept. 2005, pp. 375 –382.

[3] J. Grajal, R. Blazquez, G. Lopez-Risueno, J. Sanz, M. Burgos, and A. Asensio, "Analysis and characterization of a monobit receiver for electronic warfare," *Aerospace and Electronic Systems, IEEE Transactions on*, vol. 39, no. 1, pp. 244 – 258, jan. 2003.

[4] S. Hoyos, B. Sadler, and G. Arce, "Monobit digital receivers for ultrawideband communications," *Wireless Communications, IEEE Transactions on*, vol. 4, no. 4, pp. 1337 – 1344, july 2005.

[5] B. Murmann, "A/d converter trends: Power dissipation, scaling and digitally assisted architectures," in *Custom Integrated Circuits Conference, 2008. CICC 2008. IEEE*, sept. 2008, pp. 105 –112.

[6] M. Win and R. Scholtz, "Impulse radio: how it works," *Communications Letters, IEEE*, vol. 2, no. 2, pp. 36 –38, feb 1998.

[7] A. Trindade, Q. H. Dang, and A.-J. van der Veen, "Signal processing model for a transmit-reference uwb wireless communication system," in *Ultra Wideband Systems and Technologies, 2003 IEEE Conference on*, nov. 2003, pp. 270 – 274.

[8] S. Farahmand, X. Luo, and G. Giannakis, "Demodulation and tracking with dirty templates for uwb impulse radio: algorithms and performance," *Vehicular Technology, IEEE Transactions on*, vol. 54, no. 5, pp. 1595 – 1608, sept. 2005.

[9] M.-K. Oh, B. Jung, R. Harjani, and D.-J. Park, "A new noncoherent uwb impulse radio receiver," *Communications Letters, IEEE*, vol. 9, no. 2, pp. 151 – 153, feb. 2005.

[10] H. Yin, Z. Wang, L. Ke, and J. Wang, "Monobit digital receivers: design, performance, and application to impulse radio," *Communications, IEEE Transactions on*, vol. 58, no. 6, pp. 1695 –1704, june 2010.

[11] J. Singh and U. Madhow, "Phase-quantized block noncoherent communication," *CoRR*, vol. abs/1112.4811, 2011.

[12] B. Picinbono, "On deflection as a performance criterion in detection," *Aerospace and Electronic Systems, IEEE Transactions on*, vol. 31, no. 3, pp. 1072 –1081, jul 1995.

[13] B. Razavi, *RF microelectronics*. Upper Saddle River, NJ, USA: Prentice-Hall, Inc., 1998.

[14] A. Abidi, “Direct-conversion radio transceivers for digital communications,” *Solid-State Circuits, IEEE Journal of*, vol. 30, no. 12, pp. 1399 –1410, dec 1995.

[15] A. Tarighat, R. Bagheri, and A. Sayed, “Compensation schemes and performance analysis of iq imbalances in ofdm receivers,” *Signal Processing, IEEE Transactions on*, vol. 53, no. 8, pp. 3257 – 3268, aug. 2005.

[16] F. Gray, “Pulse code communication,” *Electrical Engineers Part IIIA Radiocommunication Journal of the Institution of*, vol. 94, no. 11, p. 83, 1953.

[17] L. Ke, H. Yin, W. Gong, and Z. Wang, “Finite-resolution digital receiver design for impulse radio ultra-wideband communication,” *Wireless Communications, IEEE Transactions on*, vol. 7, no. 12, pp. 5108 –5117, december 2008.

[18] C. Berrou, A. Glavieux, and P. Thitimajshima, “Near shannon limit error-correcting coding and decoding: Turbo-codes. 1,” in *Communications, 1993. ICC 93. Geneva. Technical Program, Conference Record, IEEE International Conference on*, vol. 2, may 1993, pp. 1064 –1070 vol.2.

[19] R. Gallager, “Low-density parity-check codes,” *Information Theory, IRE Transactions on*, vol. 8, no. 1, pp. 21 –28, january 1962.

[20] D. MacKay and R. Neal, “Near shannon limit performance of low density parity check codes,” *Electronics Letters*, vol. 33, no. 6, pp. 457 –458, mar 1997.

[21] J. Foerster, “Channel modeling sub-committee report final,” IEEE802.15-02/490, Tech. Rep., February 2003.

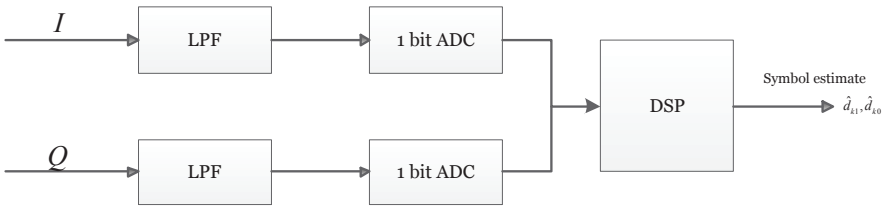

Fig. 1. Monobit receiver architecture for QPSK

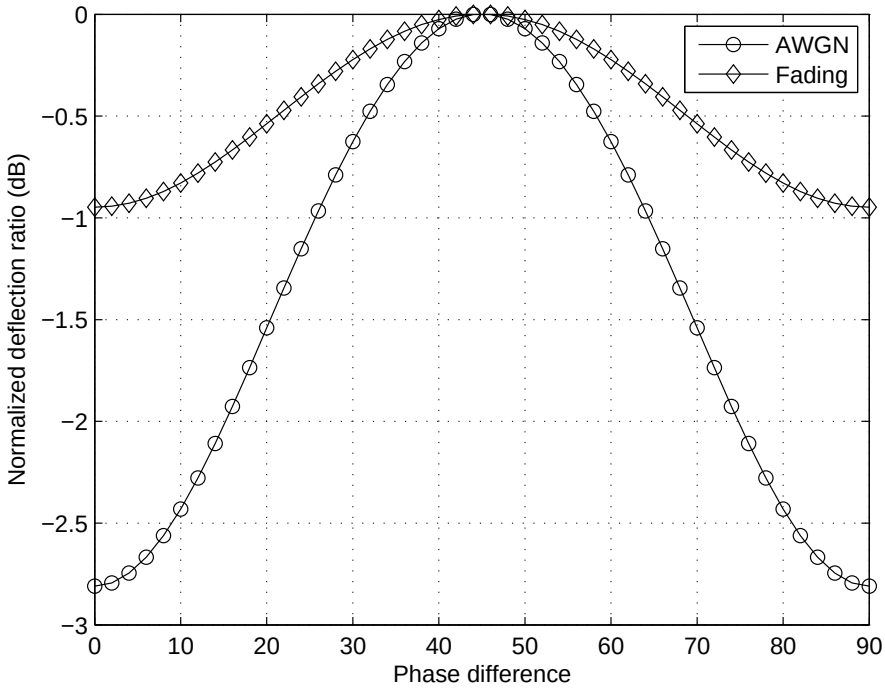

Fig. 2. Normalized deflection ratio under difference phase difference φ

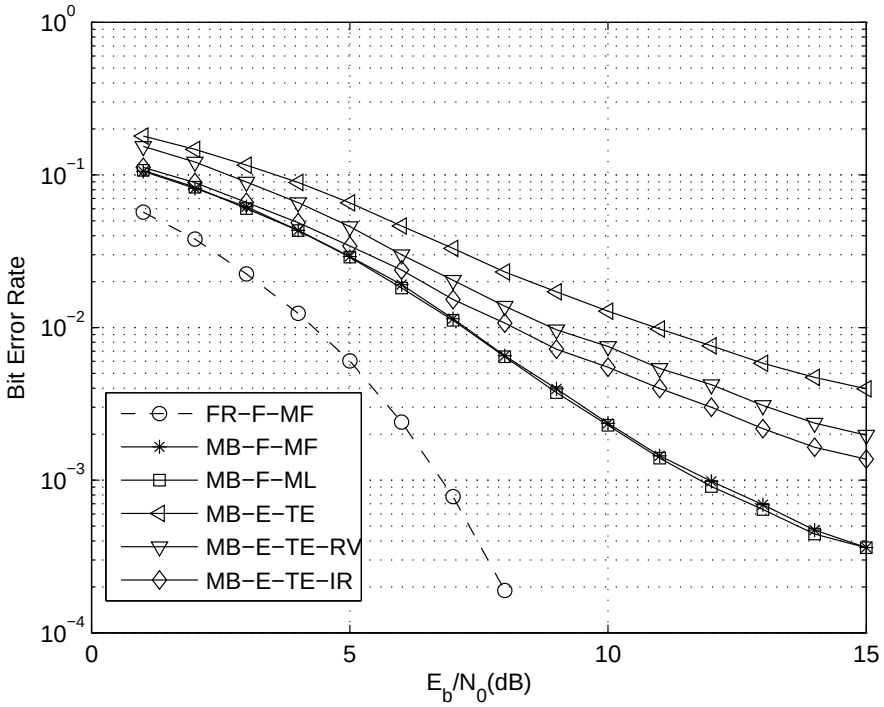

Fig. 3. Comparison of performance of optimal, suboptimal, and full-resolution, monobit receivers in AWGN channel under Nyquist sampling without IQ imbalances

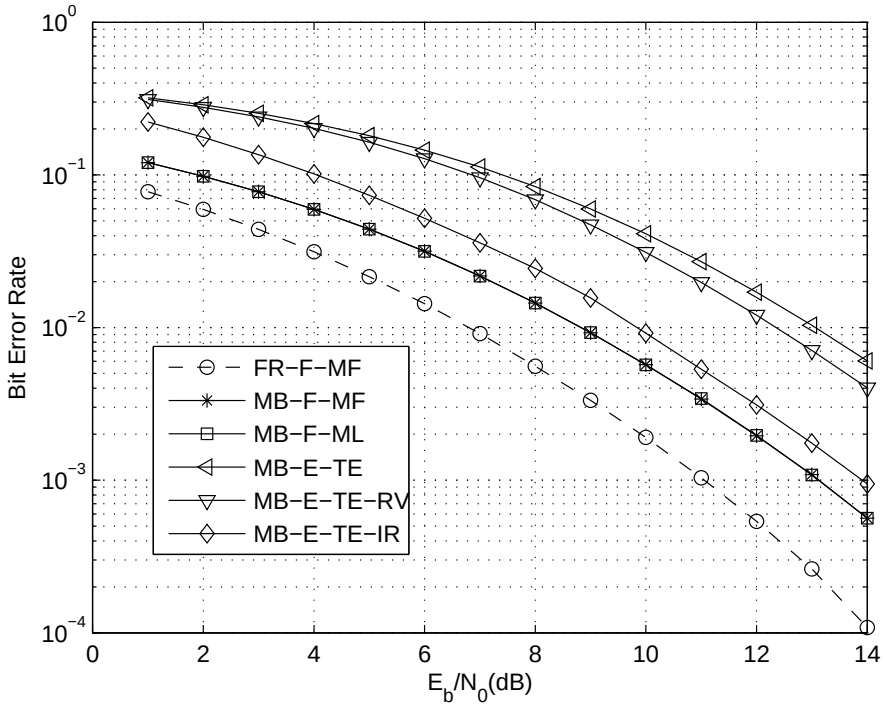

Fig. 4. Comparison of performance of optimal, suboptimal, and full-resolution, monobit receivers in fading channel under Nyquist sampling without IQ imbalances

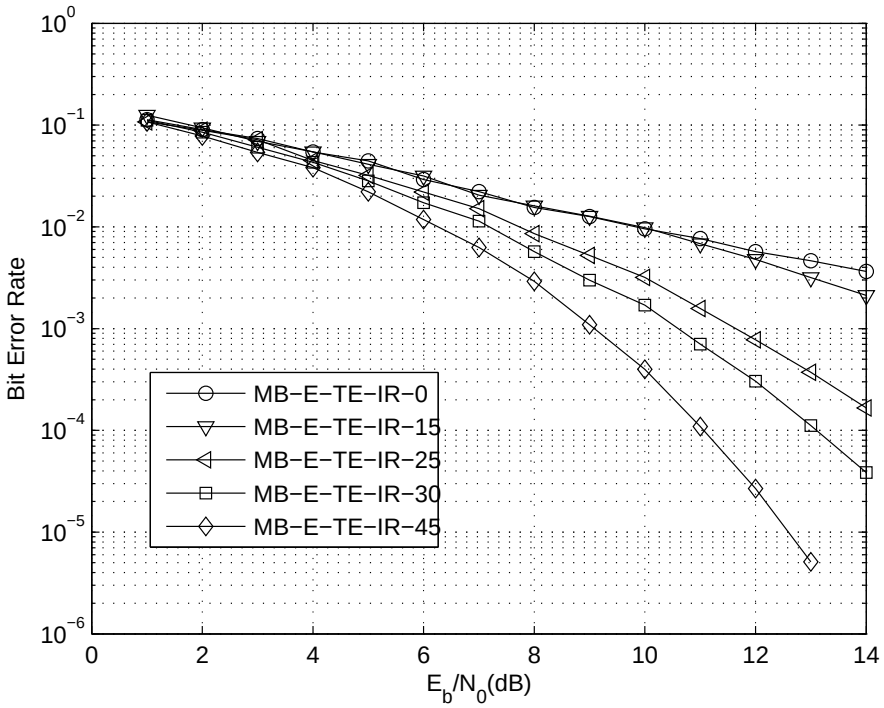

Fig. 5. Effect of phase difference on suboptimal monobit receiver in AWGN channel without IQ imbalances

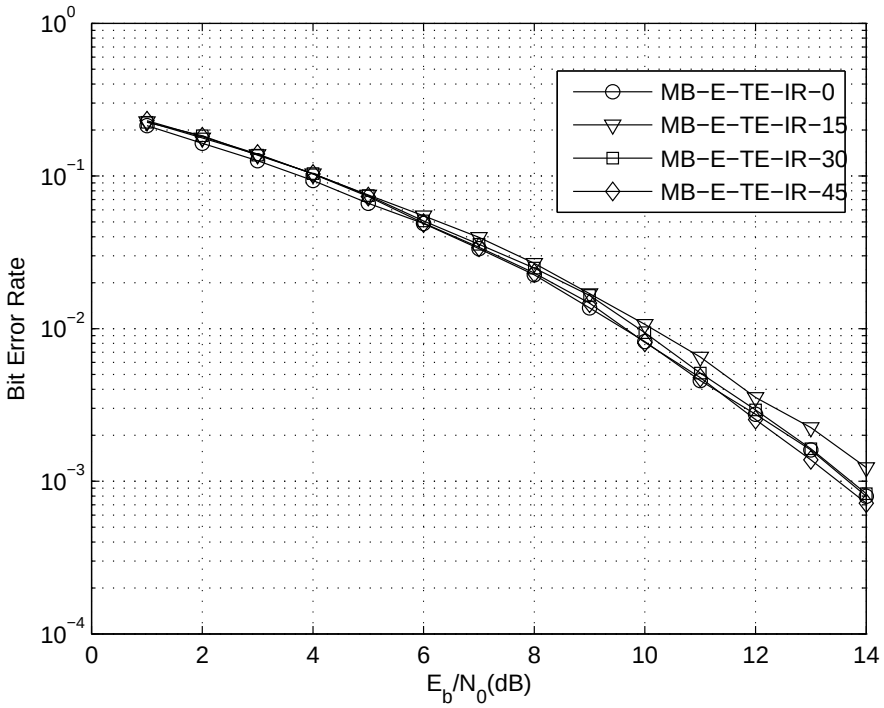

Fig. 6. Effect of phase difference on suboptimal monobit receiver in fading channel without IQ imbalances

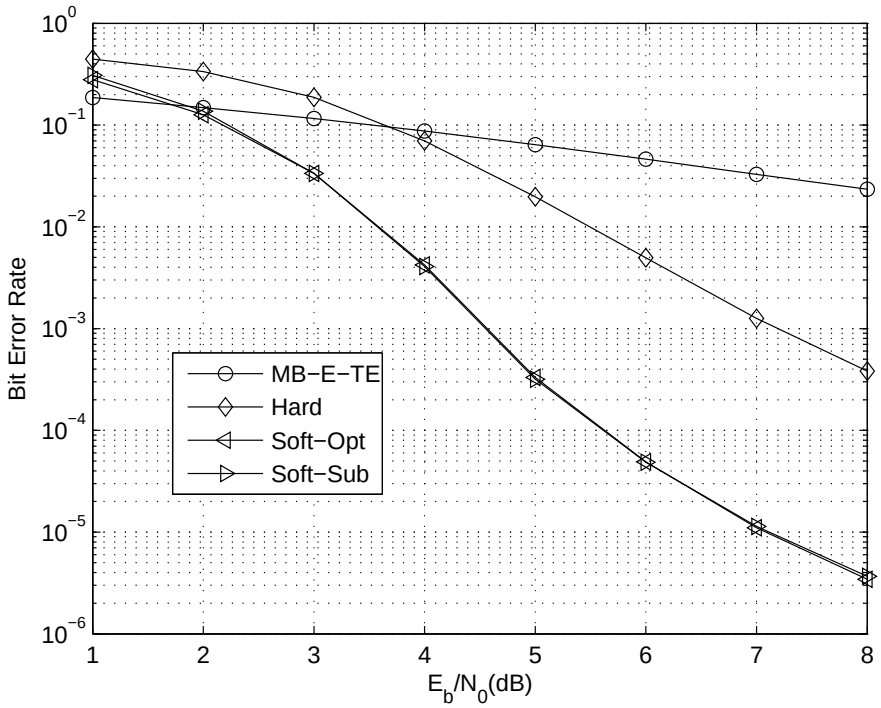

Fig. 7. Comparison of different LLR approximations for suboptimal monobit receiver in AWGN channel without IQ imbalances

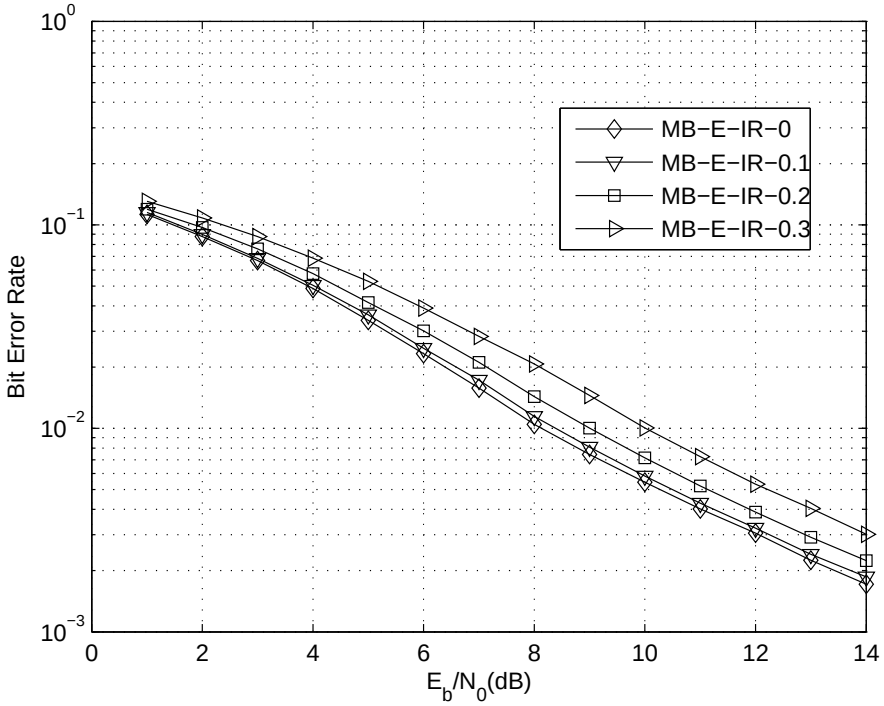

Fig. 8. Effect of the amplitude imbalance on practical monobit receiver in AWGN channel

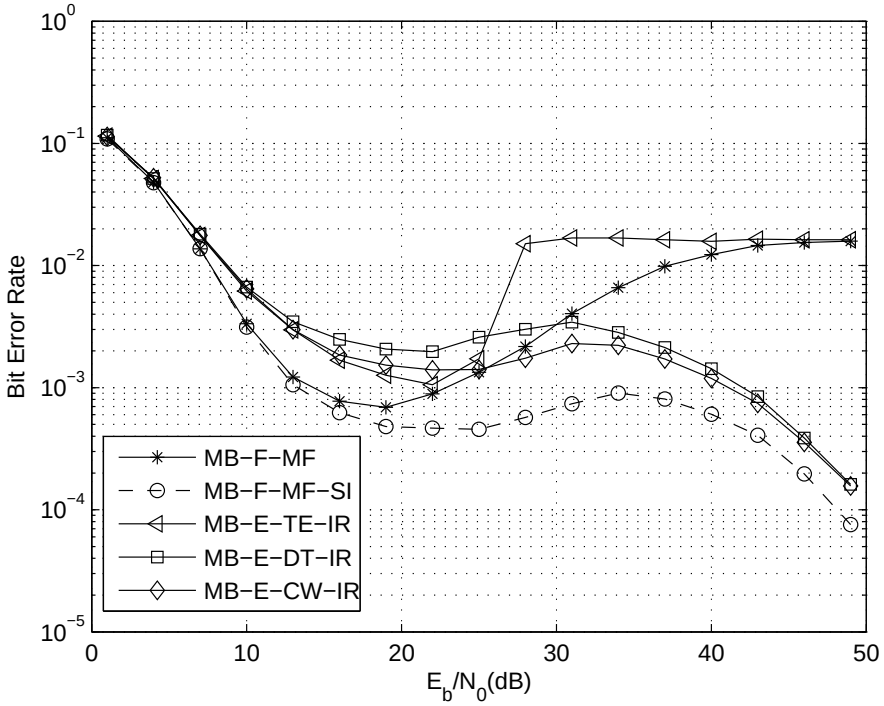

Fig. 9. Comparison of performance of different monobit receivers in AWGN channel with IQ imbalances

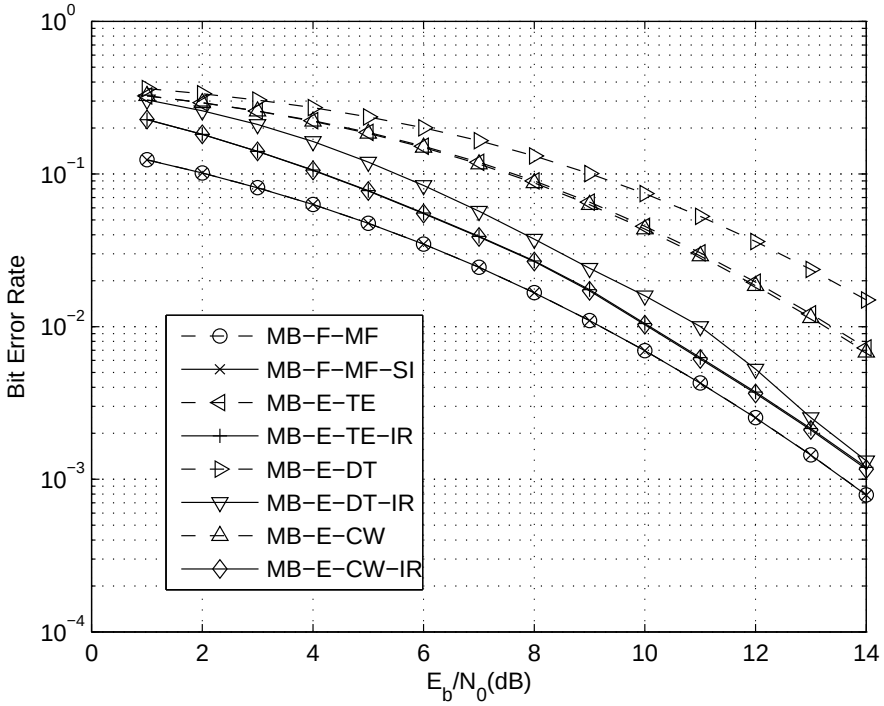

Fig. 10. Comparison of performance of different monobit receivers in fading channel with IQ imbalances

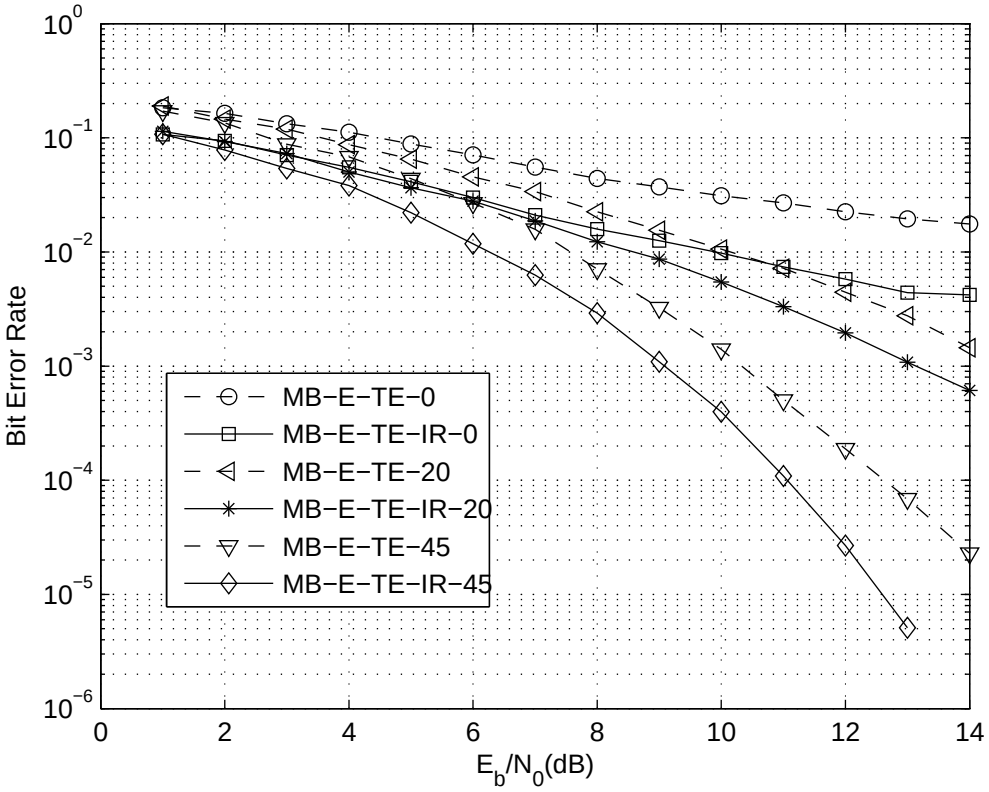
Bit Error Rate
10^{0}
10^{-1}
10^{-2}
10^{-3}
10^{-4}
10^{-5}
10^{-6}
0
2
4
6
8
10
12
14
E_b/N_0(dB)
MB−E−TE−0
MB−E−TE−IR−0
MB−E−TE−20
MB−E−TE−IR−20
MB−E−TE−45
MB−E−TE−IR−45

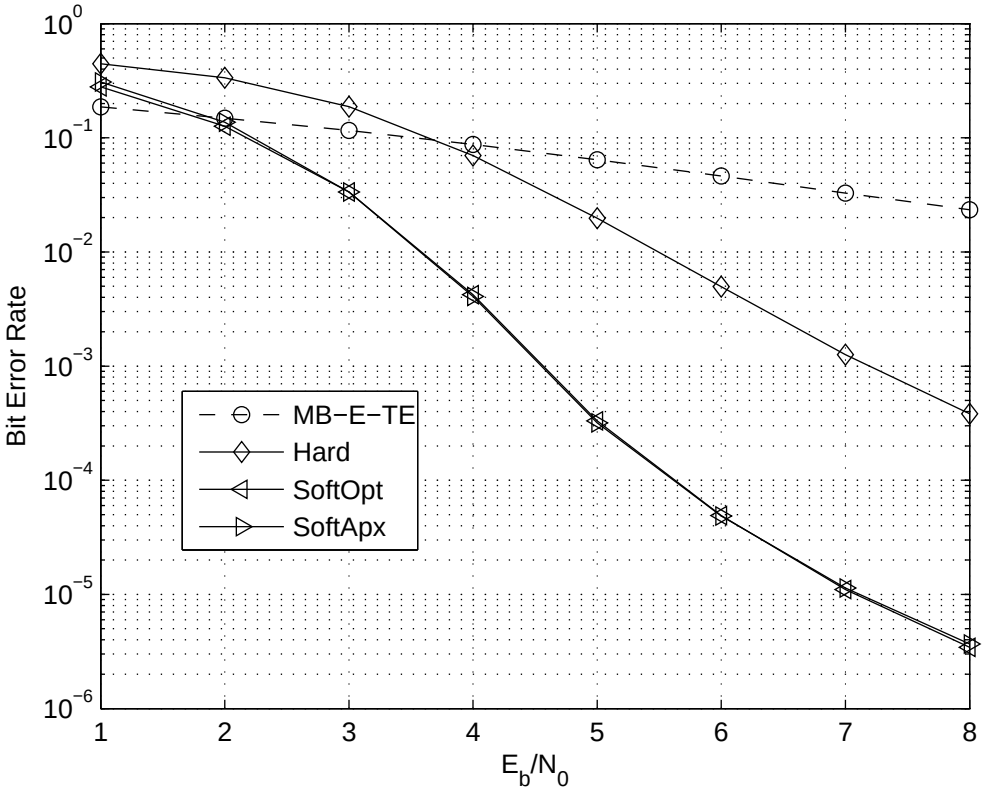
Bit Error Rate
10^{0}
10^{-1}
10^{-2}
10^{-3}
10^{-4}
10^{-5}
10^{-6}
1
2
3
4
5
6
7
8
E_b/N_0
MB−E−TE
Hard
SoftOpt
SoftApx